

Permeation of β -lactamase inhibitors through the general porins of Gram-negative bacteria

Alessandro Pira,¹ Mariano Andrea Scorciapino,² Igor V. Bodrenko,³ Andrea Bosin,¹ Silvia Acosta-Gutierrez,⁴ Matteo Ceccarelli,^{1,3,*}

¹Department of Physics and ²Department of Chemical and Geological Sciences, University of Cagliari, Cittadella Universitaria di Monserrato, S.P.8 km 0,700 – 09042 Monserrato (CA), Italy; ³CNR/IOM Sezione di Cagliari, Cittadella Universitaria, S.P. 8 km 0,700 – 09042 Monserrato (CA), Italy; ⁴Department of Chemistry, University College London - London, United Kingdom.

* To whom correspondence should be addressed

Supplementary Information

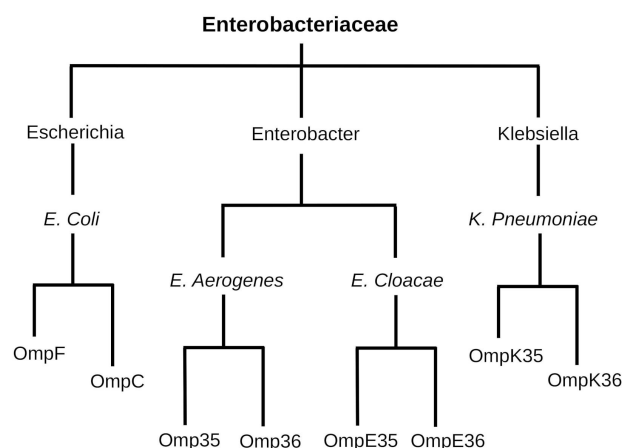


Figure S1. The *Enterobacteriaceae* family is divided into about 30 genera, among which *Escherichia*, *Enterobacter* and *Klebsiella*. In this simplified phylogenetic tree, for each of the four selected species, the two main outer membrane porins are reported. OmpF and OmpC orthologs are on the left- and on the right-hand side, respectively.

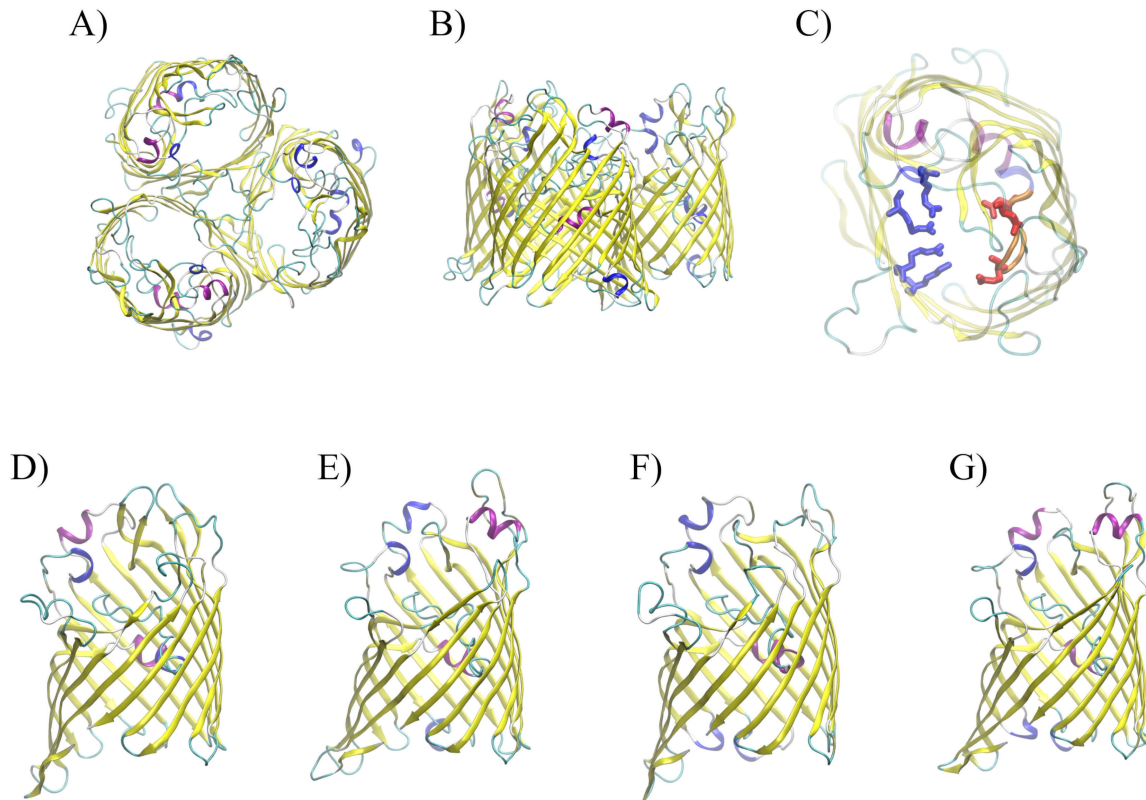


Figure S2. The OmpF trimer is shown, top-view (**A**) and side.view (**B**). One monomer is shown in (**C**), top-view, with the loop L3 highlighted, where negatively charged residues are shown in red. On the opposite side of the channel, the positively charged residues comprising the so-called basic ladder are shown in blue. This charge segregation is responsible for the intense electric field at the constriction region (CR). From (**D**) to (**G**), one monomer (side-view) of OmpF, Omp35, OmpE35 and OmpK35 is shown, respectively.

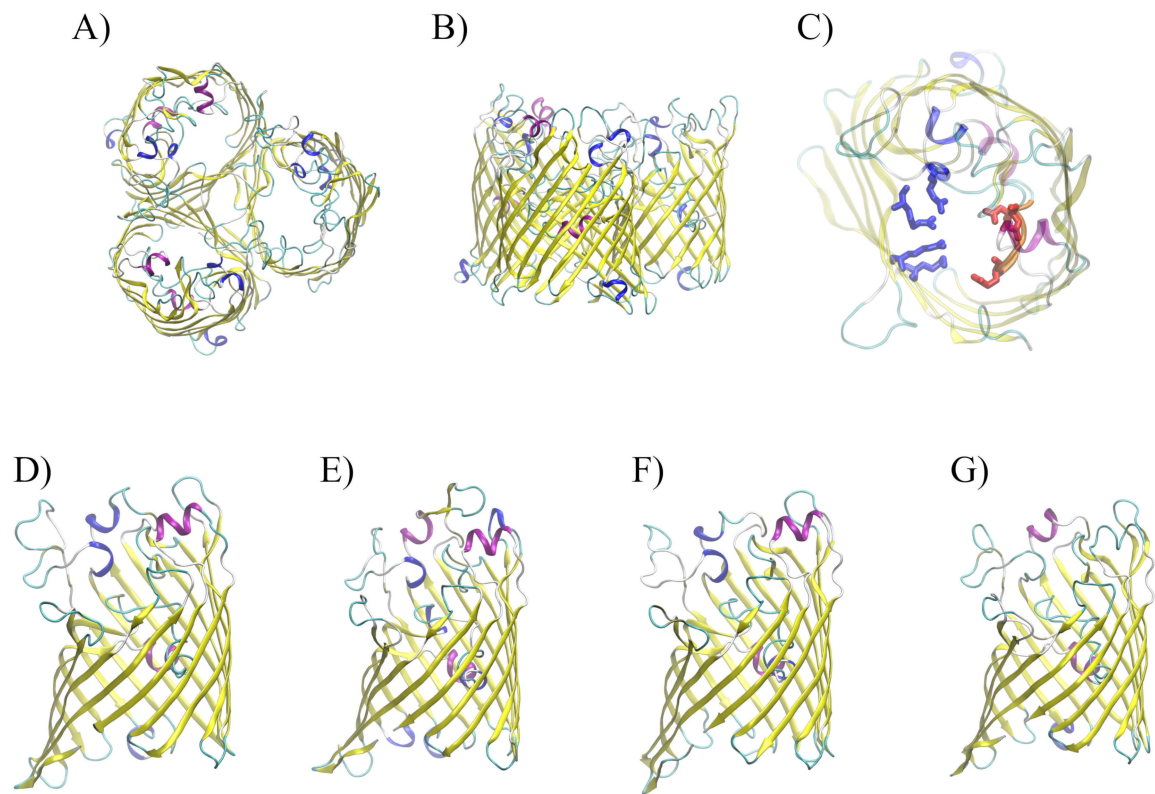


Figure S3. The OmpC trimer is shown, top-view (A) and side.view (B). One monomer is shown in (C), top-view, with the loop L3 highlighted, where negatively charged residues are shown in red. On the opposite side of the channel, the positively charged residues comprising the so-called basic ladder are shown in blue. This charge segregation is responsible for the intense electric field at the CR. From (D) to (G), one monomer (side-view) of OmpC, Omp36, OmpE36 and OmpK36 is shown, respectively.

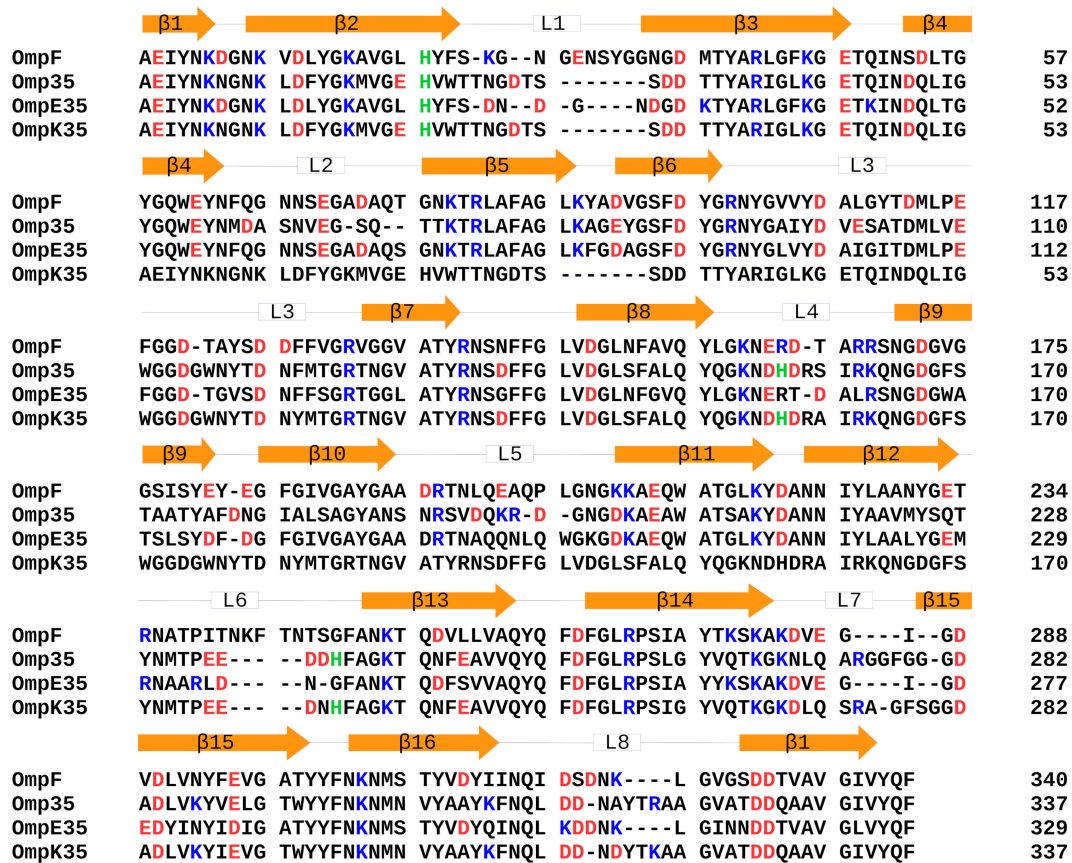


Figure S4. Structure alignment of the OmpF orthologs was obtained through the VMD software (<https://www.ks.uiuc.edu/Research/vmd/>).

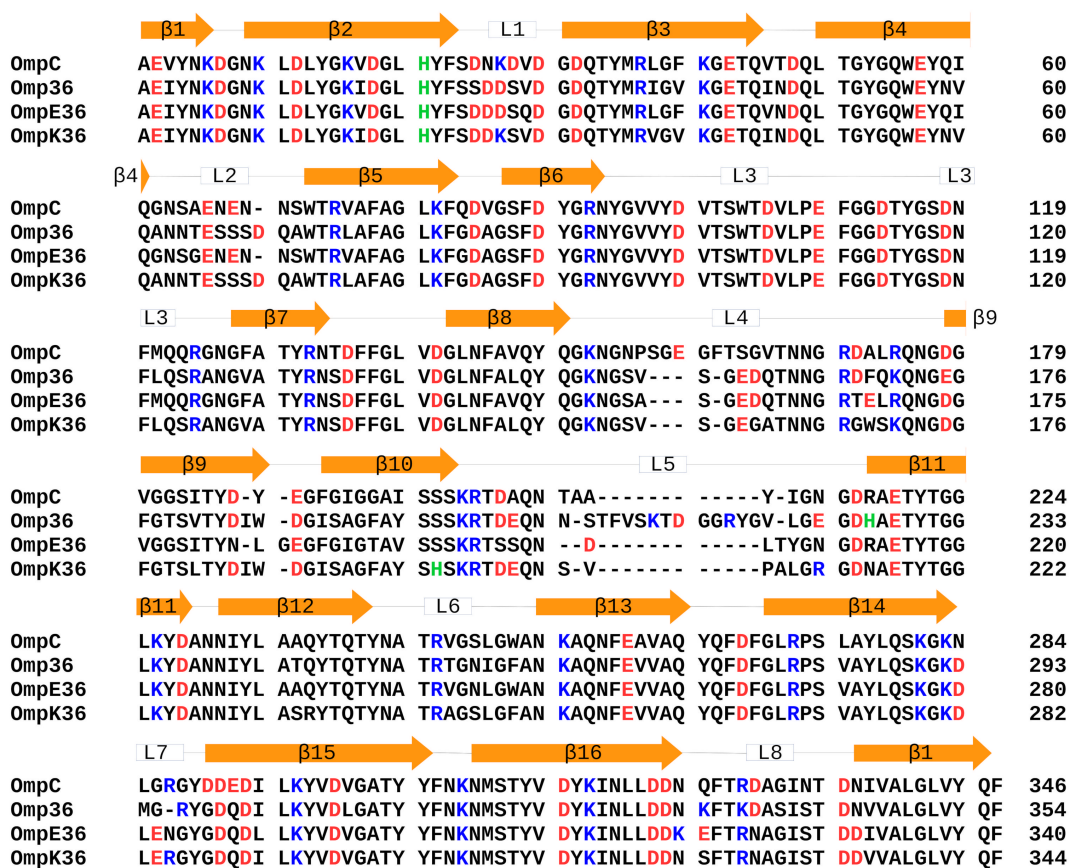


Figure S5. Structure alignment of the OmpC orthologs was obtained through the VMD software (<https://www.ks.uiuc.edu/Research/vmd/>).

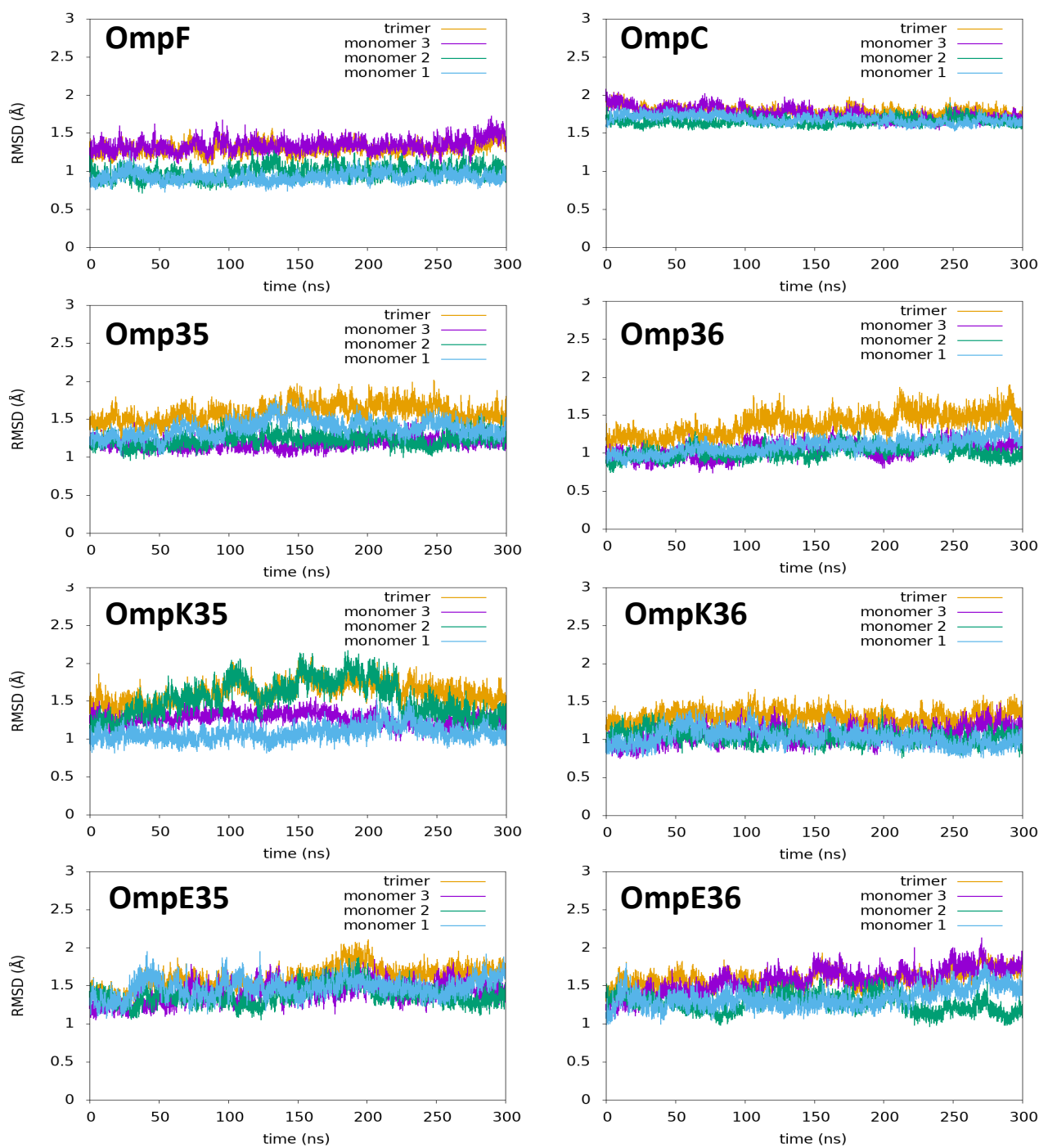


Figure S6 RMSD of the eight porins with respect to the starting X-ray structure, during the last 300 ns of equilibration simulations at 300 K in the NVT ensemble.

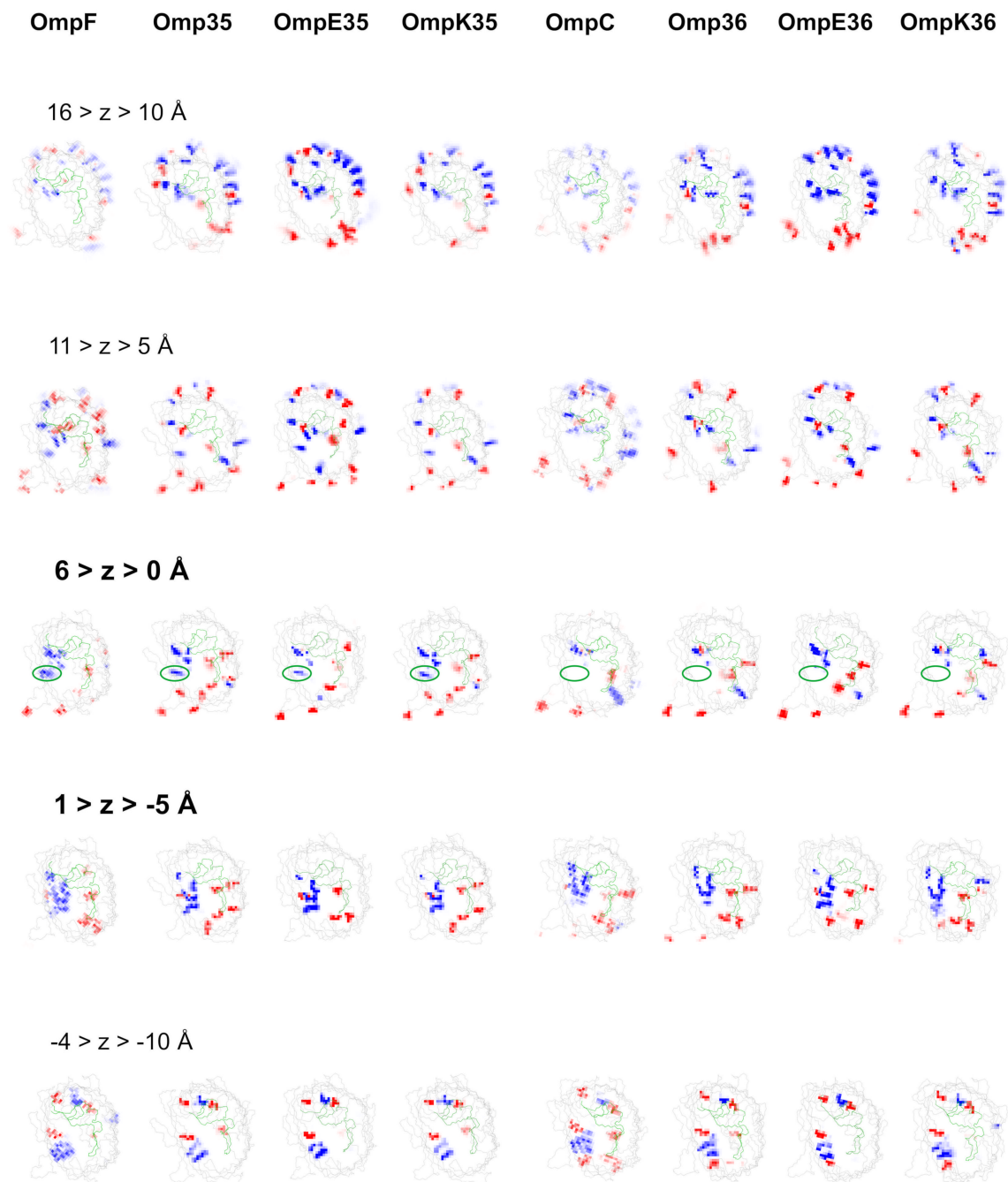


Figure S7. Distribution on the xy-plane of the difference between the density of positively and negatively charged residues, colored in blue and red, respectively. The channel was divided into 5 cross sections along the main axis, namely, $+16 \text{ \AA} > z > +10 \text{ \AA}$; $+11 \text{ \AA} > z > +5 \text{ \AA}$; $+6 \text{ \AA} > z > 0 \text{ \AA}$ (POR, the pre-orientation region); $+1 \text{ \AA} > z > -5 \text{ \AA}$ (CR, the constriction region); $-4 \text{ \AA} > z > -10 \text{ \AA}$. The circles highlight the major difference found among OmpF orthologs and OmpC orthologs.

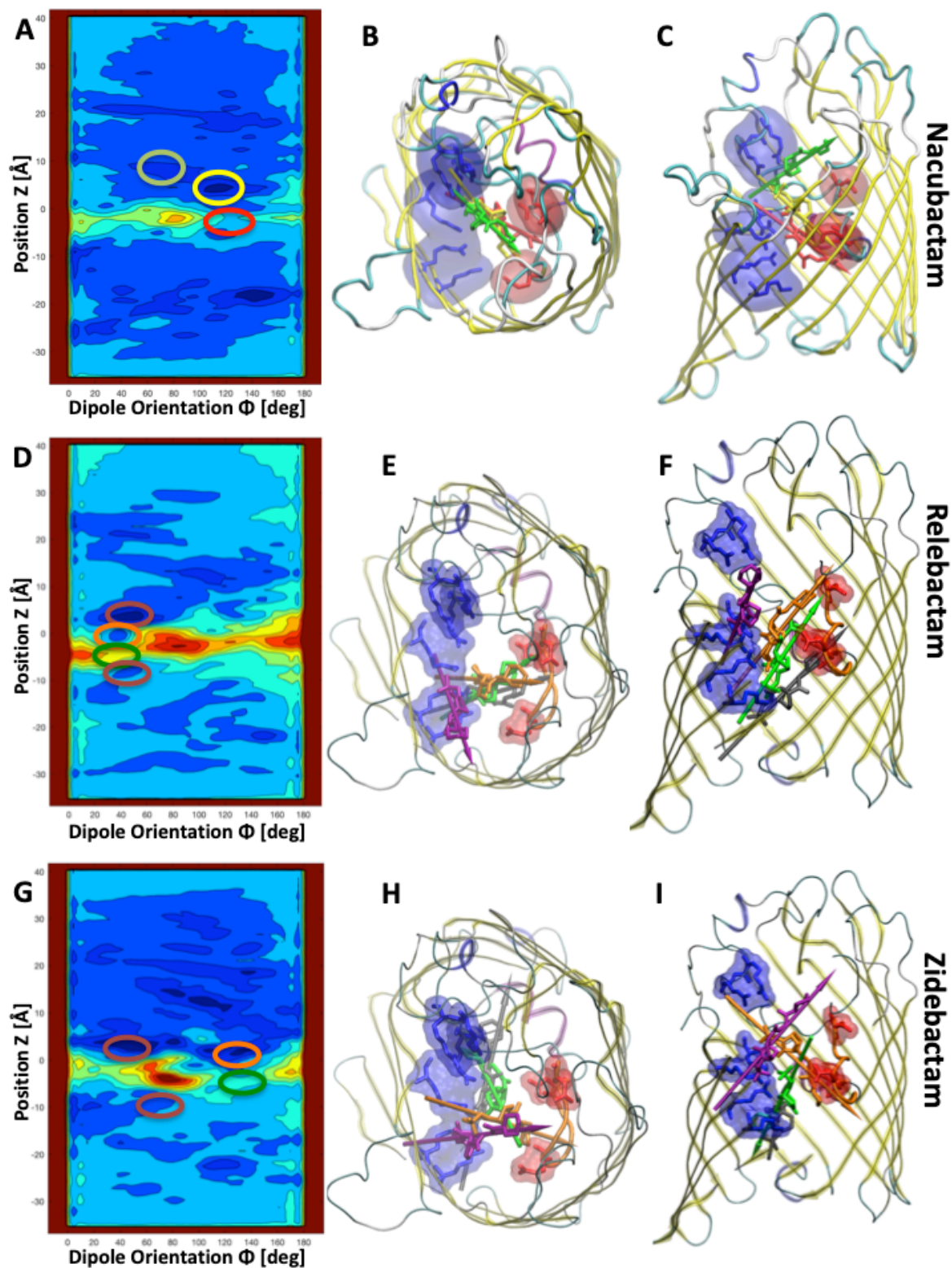


Figure S8. The same FES shown in figure 4 are reported here (A,D,G) with differently colored circles to indicate the energy minima and the saddle point analyzed along the minimum energy path in the region $10 \text{ \AA} > z > -10 \text{ \AA}$. The same colors are used to show the corresponding representative conformer of the three inhibitors under investigation together with the electric dipole. These structures are shown inside one of the monomers of OmpF from the top view (B,E,H) and side view (C,F,I).

